A Data-Driven $\mathcal{H}_2$-Optimal Control Approach for Adaptive Optics

Karel Hinnen, Michel Verhaegen, and Niek Doelman

***Abstract*—Adaptive optics (AO) is used in ground-based astronomical telescopes to improve the resolution by counteracting the effects of atmospheric turbulence. Most AO systems are based on a simple control law that neglects the temporal evolution of the distortions introduced by the atmosphere. This paper presents a data-driven control design approach that is able to exploit the spatio-temporal correlation in the wavefront, without assuming any form of decoupling. The approach consists of a dedicated subspace-identification algorithm to identify an atmospheric disturbance model from open-loop wavefront sensor data, followed by $\mathcal{H}_2$-optimal control design. It is shown that in the case that the deformable mirror and wavefront sensor dynamics can be represented by a delay and a two taps impulse response, it is possible to derive an analytical expression for the $\mathcal{H}_2$-optimal controller. Numerical simulations on AO test bench data demonstrate a performance improvement with respect to the common AO control approach.**

***Index Terms*—Adaptive optics (AO), data-driven disturbance modeling, optimal control, stochastic identification.**

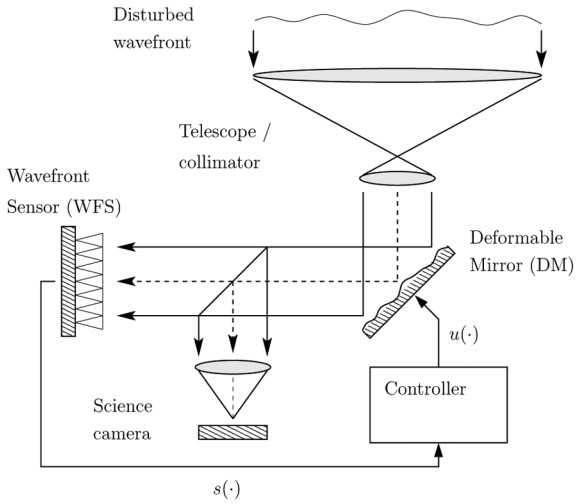

Fig. 1. Functional relationship between main components of an AO system.

I. Introduction

ADAPTIVE optics (AO) is a technique to actively sense, estimate, and correct the wavefront distortions introduced in a light beam as it propagates through a turbulent medium. It is used in ground-based astronomical imaging to overcome the loss in resolving power caused by atmospheric turbulence. Whereas atmospheric turbulence otherwise limits the angular resolution to that of an amateur telescope, AO may enable the recording of long-exposure images with resolutions close to the diffraction limit. For large 8- to 10-m telescopes this may lead to a 50$\times$ improvement in resolving power. The unprecedented resolution forms an important stimulus for astronomy and gives rise to many discoveries (see, e.g., [1]).

To explain the principle of AO, consider the AO system in Fig. 1. When light from a star arrives at the outer atmosphere it has a perfectly flat wavefront. However, space and time varying optical path length differences caused by the turbulent mixing of air, disturb the wavefront before it arrives at the telescope. The AO system uses a deformable mirror (DM) to actively control the path length differences in the system. The incoming light with an atmospherically distorted phase profile $\phi(\cdot)$ is directed to the DM, which applies a phase correction $\phi_m(\cdot)$. The reflected beam, with a residual phase error $\epsilon = \phi - \phi_m$, is then divided in two parts. The first part leaves the AO system to form an image of the science object, while the second part is directed to the wavefront sensor (WFS). The WFS provides quantitative information about the residual wavefront. Based on the WFS measurements $s(\cdot)$, the controller has to determine the DM actuator commands $u(\cdot)$. The controller should adapt the DM shape in such a way that it cancels out most of the distortions. For an extensive overview of field of AO, the reader is referred to [2]–[4].

This paper focuses on the control aspects of AO. A common measure of the performance in AO is the Strehl ratio, which is defined as the on-axis intensity of a point source relative to that of the diffraction limit. Through the Marechal approximation [5], maximizing the Strehl is equivalent to minimizing the mean-square error (MSE) of the phase. The AO control problem can hence be formulated as finding the controller that minimizes the mean-square residual wavefront. An important complication is that the WFS is not able to directly measure the phase but typically provides some measure of the slope of the wavefront. The common way to deal with this discrepancy is to include a separate wavefront reconstruction step. Given the reconstructed wavefront, the problem of imposing the proper shape on the DM is seen as a servo control problem. As a result, the majority of the AO systems are based on a control law that consists of a static

Manuscript received March 20, 2006; revised January 4, 2007. Manuscript received in final form April 12, 2007. Recommended by Associate Editor D. Gorinevsky. This work was supported by TNO Science and Industry, Delft, The Netherlands.

K. Hinnen is with the Delft Center for Systems and Control, Delft University of Technology, Mekelweg 2, 2628 CD Delft, The Netherlands (e-mail: k.j.g.hinnen@planet.nl).

M. Verhaegen is with the Delft Center for Systems and Control, Delft University of Technology, Mekelweg 2, 2628 CD Delft, The Netherlands.

N. Doelman is with the TNO Science and Industry, 26 AD Delft, The Netherlands.

Color versions of one or more of the figures in this paper are available online at http://ieeexplore.ieee.org.

Digital Object Identifier 10.1109/TCST.2007.903374

wavefront reconstruction step, the projection of the estimated wavefront on the DM actuator space and a dynamic servo compensator responsible for stability and closed-loop performance [4], [6].

In the simplest case, the wavefront reconstructor and the DM fitting matrix are obtained as the pseudo-inverse of the phase-to-slope mapping and the DM influence matrix. Both maximum likelihood and maximum *a posteriori* techniques have been used to improve the estimate by incorporating prior knowledge on the second order statistics of the spatial distribution of the wavefront [4], [7]. The modified statistics due to closed-loop operation, are often neglected. In designing the dynamic servo controller, it is typically assumed that the control loop can be decoupled in a series of independent single-input–single-output (SISO) feedback loops. Common servo controller structures include the leaky integrator, the proportional-integral (PI) controller and the Smith predictor. The choice of the control parameters is a trade off between disturbance rejection, noise propagation, and closed-loop stability. The higher the control bandwidth, the better the disturbance rejection but also the higher the noise propagation and risk of instabilities. In the modal control optimization approach [8], [9], the wavefront is decomposed on a set of basis functions and the gain of each mode is optimized separately.

Even though the common AO control strategy already does a remarkable job, there is still a need for improvement. As pointed out by Roddier [10], the compensation efficiency of large AO systems is unduly low, and rather than focusing only on systems with more sensors and actuators, it may be rewarding to search for ways of improving the performance of current systems. It is clear that the common AO control approach does not explicitly account for the temporal evolution of the wavefront and the dynamics of the AO system, while the time delay between measurement and correction is known to be one of the dominant error sources [6], [11]. A promising way to reduce the effect of the temporal error is to exploit the temporal correlation to anticipate future wavefront distortions. In the spirit of modal optimization, a modal linear predictive controller, whose parameters are optimized by recursive least-squares, has been introduced [11]. Since this approach assumes modal decoupling, it is still not able to take full advantage of the spatio-temporal correlation in the wavefront.

This paper presents a data-driven control design approach that takes advantage of the spatio-temporal correlation. In contrast to the previous approaches, it does not assume any form of decoupling between the spatial and temporal dynamics. The proposed control design approach consists of two steps (block 1 and 2 in Fig. 2). In the first step, a dedicated subspace identification algorithm is used to identify a multivariable atmospheric disturbance model on the basis of open-loop WFS data. The identified atmospheric disturbance model is then used to compute the optimal controller by formulating the AO control problem in an $\mathcal{H}_2$-optimal control framework. The $\mathcal{H}_2$-optimization problem is equivalent to linear quadratic Gaussian (LQG) control design, but provides a more elegant framework for formulating the discrepancy between measurement and control objective. The LQG framework has been used by Paschall and Anderson [12] to design an AO controller under the simplifying assumption that the first 14 Zernike modes of the atmospheric wavefront distortions

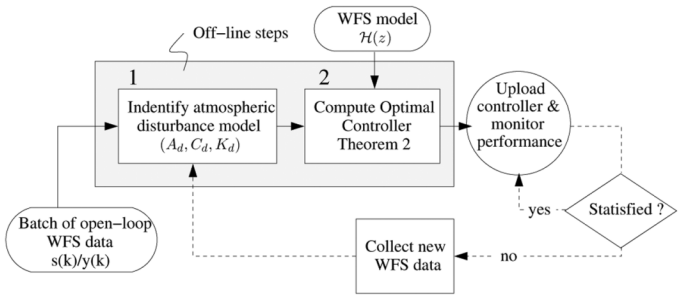

Fig. 2. Flowchart of control strategy. This paper discusses the identification and controller design steps (shaded box). To guarantee a good performance over long time scales an updating scheme might be necessary (dashed lines).

can be described by independent first-order Markov processes. Looze *et al.* [13] have used LQG to design a diagonal modal controller based on an atmospheric disturbance model in which each individual modes is described by an autoregressive moving average (ARMA) model. The LQG control approach has proven to be suitable for both classical and multiconjugated AO systems [14]. Since each of these LQG approaches assumes either modal decoupling or uses only a first-order autoregressive (AR) atmospheric disturbance model, they are not able to exploit the spatio-temporal correlation imposed by for instance the Taylor hypothesis [2], [4]. From the Taylor hypothesis, which states that the atmospheric turbulence evolves at a time-scale much longer than the time it takes for the inhomogeneities to cross the line of sight, it is clear that the upper wind WFS channels provide direct information on the future development of the turbulence elsewhere in the aperture. Gavel and Wiberg [15], recently proposed an optimal control approach which is explicitly based on the Taylor hypothesis. A disadvantage of this approach is that the Taylor hypothesis may only be partially satisfied in practice.

The proposed control approach is sufficiently general to exploit the spatio-temporal correlation imposed by the Taylor hypothesis, but does not depend on it. Furthermore, the data-driven modeling approach has the advantage that it yields a good match with the prevalent turbulence conditions and it does not require accurate estimates of physical parameters like the wind speed of the frozen layers. Apart from using a more general atmospheric disturbance model, this paper shows that the special structure of the AO control problem can be exploited in computing the $\mathcal{H}_2$-optimal controller. In general, computing the optimal controller requires the numerical solution of two Riccati equations. Since the number of channels in an AO system is large, this may be computationally demanding [13]. Due to the special structure of the identified disturbance model, in the worst case only one Riccati equation needs to be solved. Furthermore, it will be shown that in certain cases an analytical expression can be derived.

The remainder of this paper is organized as follows. Section II provides an accurate description of the AO control problem. The subspace identification algorithm used to obtain a control-relevant atmospheric disturbance model from open-loop wavefront sensor data is considered in Section III. Given the identified disturbance model, Section IV considers how to compute the $\mathcal{H}_2$-optimal controller using the special structure of the AO

problem. Section V presents a validation study in which the performance of the proposed control strategy is compared with the common AO control law. The simulations are performed on the basis of open-loop WFS data obtained from an AO test bench. Section VI concludes this paper.

II. AO Control Problem

In this paper, it will be assumed that the phase distortion profile over the aperture can be represented by a finite-dimensional discrete-time vector signal. At each discrete time instant $k \in \mathbb{N}$, the uncorrected wavefront, the DM phase correction, and the residual wavefront error are described by the vectors $\phi(k) \in \mathbb{R}^{m_\phi}$, $\phi_m(k) \in \mathbb{R}^{m_\phi}$, and $\epsilon(k) \in \mathbb{R}^{m_\phi}$. Whether the vectors provide a zonal or modal description of the wavefront is irrelevant as long as its mean-square error provides a good approximation of the mean-square wavefront over the aperture. An important complication in AO is that the wavefront distortion $\phi(k)$ cannot be measured directly. Only the WFS slope measurements $s(k) \in \mathbb{R}^{m_s}$ are available for identification and control. It is generally not possible to reconstruct the entire wavefront from $s(k)$. To arrive at a well-posed control and identification problem it is important to exclude the part of $\phi(k)$ that cannot be reconstructed. This is achieved by introducing a signal of lower dimension.

The block scheme in Fig. 3 illustrates the relation between the physical signals and their reduced counterpart. The reduced representation is obtained by considering the WFS model

$$s(k) = \mathcal{G}\phi(k) + \eta(k) \tag{1}$$

where $\mathcal{G}(z) = g(z)G$ is the cascade of a scalar linear time invariant (LTI) system $g(z)$, which accounts for the WFS dynamics, and a geometry matrix $G \in \mathbb{R}^{m_s \times m_\phi}$, which describes the optical transformation from phase to slopes. The additive term $\eta(\cdot)$ represents the measurement noise and is assumed to be zero-mean, white, and uncorrelated with $\phi(k)$. From (1), it is clear that only the part of the wavefront that is in the row space of G can be reconstructed from $s(k)$. The part of $\phi(k)$ that is in the null space of G does not contribute to $s(k)$ and can hence never be reconstructed. A reduced basis for the observable part of $\phi(k)$ can be obtained by considering the singular value decomposition (SVD)

$$G = U\Sigma V^T = [\,U_1 \quad U_2\,] \begin{bmatrix} \Sigma_1 & 0 \\ 0 & 0 \end{bmatrix} \begin{bmatrix} V_1^T \\ V_2^T \end{bmatrix}$$

where U and V are orthonormal matrices and the partitioning of $\Sigma \in \mathbb{R}^{m_s \times m_\phi}$ is such that $\Sigma_1 \in \mathbb{R}^{m_y \times m_y}$ contains all nonzero singular values. Substituting the SVD in (1) and premultiplying both sides with U_1^T, gives the reduced WFS model

$$y(k) = \Sigma_1 \varphi(k) + n(k) \tag{2}$$

where $y(k) \doteq U_1^T s(k) \in \mathbb{R}^{m_y}$, $\varphi(k) \doteq g(z)V_1^T\phi(k) \in \mathbb{R}^{m_y}$, and $n(k) \doteq U_1^T\eta(k) \in \mathbb{R}^{m_y}$. The signal $\varphi(k)$ can be interpreted as a filtered reduced representation of the observable part of $\phi(k)$. This can be seen by noting that due to the orthogonality of V, $\phi(k)$ can be decomposed as $\phi(k) = V_1V_1^T\phi(k) + V_2V_2^T\phi(k)$. Whereas the first term has a direct influence on $s(k)$, the second term does not contribute as it lies in the null-space of G. Furthermore, it is clear that the signals $g(z)\phi(k)$ and $\varphi(k)$ have the same 2-norm. Hence, $y(k)$ can be regarded as a reduced representation of the informative part of $s(k)$, while $n(k)$ denotes the measurement noise in the range space of G. The part of $\eta(k)$ that is not in the range space of G can never be caused by the wavefront distortions and is removed by the projection U_1^T. Since G is generally tall, the reduced representation leads to a reduction of the dimension of the signal that has to be modeled.

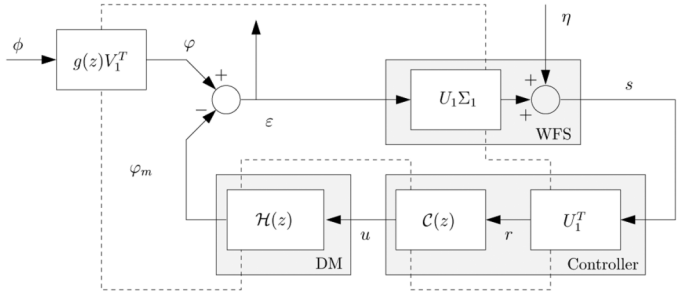

Fig. 3. Block scheme of closed-loop AO system. The dashed lines denote the borders between physical signals and the reduced signals.

In accordance with the previous definitions, the reduced representation of the applied phase correction and residual phase error are defined as $\varphi_m \doteq g(z)V_1^T\phi_m$ and $\varepsilon(k) \doteq \varphi(k) - \varphi_m(k)$. Linearity of the WFS implies that the reduced WFS signal corresponding $\varepsilon(k)$ can be expressed as $r(k) \doteq y(k) - y_m(k)$, where $y(k)$ and $y_m(k)$ denote the contributions due to atmospheric turbulence and the DM. It will be assumed that the relation between the actuator inputs $u(k) \in \mathbb{R}^{m_u}$ and the DM wavefront correction $\varphi_m(k) \in \mathbb{R}^{m_y}$, can be described by a LTI system with state-space realization

$$\mathcal{H}(z) = C_m(zI - A_m)^{-1}B_m. \tag{3}$$

The absence of a direct feed-through term in the DM model is not restrictive as there is always at least one sample delay between measurement and correction. Without loss of generality this delay can be included in the DM model. Furthermore, note that by the definition of $\varphi(k)$ the WFS dynamics $g(z)$ are implicitly included in the DM model. Because of this, (2) is free of any dynamics. The reason for this choice will be discussed after defining the cost function in (5).

Optimizing the AO system performance requires accurate knowledge of the statistical properties of the uncorrected wavefront. The basic assumption in this paper is that the uncorrected wavefront $\varphi(k)$, and hence also $y(k)$, can be modeled as a regular process. This is to say that the second-order statistics of these signals are modeled as the output of an LTI system with a zero-mean white noise input. The assumption of stationarity is implicit in most AO literature and the proposed control strategies are typically not able to respond to changes in the turbulence statistics. An exception to this is formed by the class of adaptive control approaches to AO (see, e.g., [16]). Modeling the wavefront distortions as a regular stochastic process is reasonable on sufficiently short time-scales as the statistical properties of the turbulence evolve much slower than the wavefront fluctuations themselves. To guarantee a good

performance over longer time periods, it is necessary to update the disturbance model on a regular basis. This represented schematically by the update loop in Fig. 2. Such a model updating scheme can for instance be used to deal with gradual changes in the wind speed and wind direction. Fast changes, like wind gusts, on the other hand can only be accounted for in a stochastic setting by regarding them as a part of the stochastic distortion. In fact, wind gusts may be seen as one of the driving forces of atmospheric turbulence.

Without loss of generality, it will be assumed that the atmospheric disturbance model is in innovation form [17] with respect to $y(k)$. This in combination with (2) gives rise to the model structure

$$\mathcal{S}: \begin{cases} x(k+1) = A_d x(k) + K_d v(k) \\ y(k) = \Sigma_1 C_d x(k) + v(k) \\ \varphi(k) = C_d x(k) + \zeta(k) \end{cases} \tag{4}$$

where $A_d - K_d \Sigma_1 C_d \in \mathbb{R}^{n_d \times n_d}$ and $A_d \in \mathbb{R}^{n_d \times n_d}$ are stable, and $v(k) \in \mathbb{R}^{m_y}$ is a zero-mean white process with covariance $R_v \doteq \mathcal{E}\{v(k)v^T(k)\}$. Also, the signal $\zeta(k) \doteq \Sigma^{-1}(v(k) - n(k))$ is zero-mean and white. Its covariance and cross-covariance with $v(k)$, respectively, are denoted by $R_\zeta \doteq \mathcal{E}\{\zeta(k)\zeta(k)^T\}$ and $R_{v\zeta} \doteq \mathcal{E}\{v(k)\zeta(k)^T\}$. The atmospheric disturbance model is assumed to be minimal in the sense that output signals cannot be described by an LTI model of order less than n_d. In this way, $\mathcal{S}$ provides a minimum-phase spectral factor of the stochastic process $y(k)$, which will appear to be a very useful property in computing the optimal controller. Note that since the atmospheric disturbance model is in innovation form with respect to $y(k)$, the innovations process $v(k)$ incorporates both the effect of atmospheric turbulence and measurement noise. From the WFS model (2), however, it is clear that by the definition of $\zeta(k)$, the signal $\phi(k)$ becomes independent from the measurement noise $n(k)$, as it should.

The problem considered in this paper can be divided into two parts. Given a batch of $N_i \in \mathbb{N}$ open-loop WFS observations $y(k)$, the first subproblem is to estimate the system matrices $A_d \in \mathbb{R}^{n_d \times n_d}$, $K_d \in \mathbb{R}^{n_d \times m_y}$, and $\Sigma_1 C_d \in \mathbb{R}^{m_y \times n_d}$. This part of the problem is referred to as the stochastic identification problem. After identifying the system matrices of $\mathcal{S}$, the second subproblem is to find the optimal controller $\mathcal{C}(z)$ that minimizes the cost function

$$J = \mathcal{E}\left\{\varepsilon^T(k)\varepsilon(k)\right\} + \mathcal{E}\left\{u^T(k)Qu(k)\right\} \tag{5}$$

where $Q \geq 0$ is a regularization matrix which makes a tradeoff between the expected mean-square residual phase error $\mathcal{E}(\varepsilon^T(k)\varepsilon(k))$ and the expected amount of control effort $\mathcal{E}(u^T(k)u(k))$. By increasing the control effort weighting Q it is possible to reduce the amount of energy dissipated by the DM and make the controller more robust to model uncertainties. The matrix Q will be typically chosen diagonal, allowing for a penalty on the control effort on each of the actuators separately. Furthermore, it is important to recall that signal $\varepsilon(k)$ has been defined in such a way that it incorporates the WFS dynamics $g(z)$. Minimizing the first term of (5) is therefore equivalent to minimizing the mean-square error of the observable part of the filtered signal $g(z)\epsilon(k)$. Even though it is possible to explicitly account for the WFS dynamics in the definition of cost function, this is usually not sensible because the WFS usually has low-pass characteristics. This implies that the WFS dynamics mainly distorts the high frequency region of ε, while the turbulence is dominant at the low frequencies. Moreover by inverting the WFS dynamics one risks the chance of high-frequency noise amplification.

III. Data-Driven Disturbance Modeling

In this section, we present a dedicated subspace identification algorithm that is able to deal with the stochastic identification problem. Based on open-loop WFS data $y(k)$, the algorithm provides a full atmospheric disturbance model $\mathcal{S}$, without assuming any form of decoupling between the channels. A consequence of this extensive description is that even for small AO systems a huge identification problem has to be solved. Computational efficiency is therefore an important issue.

Based on numerically robust matrix operations, subspace algorithms bypass the need for model parameterization and nonlinear optimization. This is an important advantage over the more traditional maximum likelihood and prediction error methods [18], which rely on the optimization of a cost function of model parameters. Apart from the risk of ending up in a local minimum, the computational complexity of these algorithm grows rapidly with the number of parameters. This is especially a problem in the multivariate case where the mapping from each input to each output is often parametrized independently. With subspace identification, the multivariate case can be handled within the same framework.

The subspace identification algorithm presented in this paper is basically an efficient output only implementation of the SSARX algorithm [19]. In analogy with the name SSARX, the new algorithm will be called SSAR. An important advantage of the algorithm is that it provides a direct estimate of the state-space matrices of the minimum-phase spectral factor. Most subspace identification algorithms for stochastic identification, are based on a two-step procedure where the minimum-phase spectral factor is obtained after the factorization of some intermediate estimate. Apart from the fact that such a two-step procedure is computationally more complex, it has the disadvantage that the spectral factorization might fail to have a solution. The class of subspace algorithms that first estimate a rational covariance model [20] is an example of this. As demonstrated in [21], the spectral factorization problem has only a solution when the rational covariance model is positive real. The SSAR algorithm avoids the need for spectral factorization by directly estimating the system matrices of the Kalman predictor model. The minimum-phase requirement is translated to a stability requirement on the system matrices of the Kalman filter and the minimum-phase spectral factor. This requirement can be easily checked and if necessary enforced by using the Schur restabilization procedure in [22].

In estimating the state sequence, the proposed subspace algorithm uses a weighting scheme that differs from SSARX. In this way, a single RQ factorization of a stacked block-Hankel matrix of past and future data can be used both for computing the required AR coefficients and for data compression. This leads to an efficient implementation both in terms of the number of flops

and the memory requirements. Before providing a detailed description of SSAR, the SSARX algorithm in [19] will be briefly reviewed. This will prove to be valuable for explaining the algorithm and in outlining the difference with an output only implementation of SSARX.

The SSARX algorithm is based on an alternative representation of the stochastic process $y(k) \in \mathbb{R}^{m_y}$. Consider the stochastic disturbance model (4). By using the output equation to eliminate the noise input $v(k) \in \mathbb{R}^{m_y}$ from the state-update equation, the stochastic process $y(k)$ can be represented as

$$\widetilde{\mathcal{S}} : \begin{cases} x(k+1) = \widetilde{A}x(k) + \widetilde{K}y(k) \\ y(k) = \widetilde{C}x(k) + v(k) \end{cases} \tag{6}$$

where $\widetilde{A} \doteq A_d - K_d\widetilde{C}$, $\widetilde{C} \doteq \Sigma_1 C_d$, and where $\widetilde{K}$ is defined as $\widetilde{K} \doteq K_d$ to achieve uniformity in notation. The previous representation of $y(k)$ can be seen as the Kalman predictor model corresponding to (4). Furthermore, it is clear that the minimum-phase requirement on the stochastic disturbance model is equivalent to demanding that $\widetilde{A}$ is asymptotically stable. Let the vectors of past and future outputs and future innovations be defined as

$$\begin{aligned} y_p(k-p) &\doteq [\, y^T(k-p) \quad \dots \quad y^T(k-2) \quad y^T(k-1)\,]^T \\ y_f(k) &\doteq [\, y^T(k) \quad y^T(k+1) \quad \dots \quad y^T(k+f-1)\,]^T \\ v_f(k) &\doteq [\, v^T(k) \quad v^T(k+1) \quad \dots \quad v^T(k+f-1)\,]^T \end{aligned}$$

with $p, f \in \mathbb{N}$ some user defined parameters, whose selection will be discussed later on. Then, by iteratively applying the state-update equation in (6), it can be shown [19], [23] that if p is sufficiently large, the state $x(k)$ can be approximated as

$$x(k) \approx \mathcal{K}_p y_p(k-p) \tag{7}$$

where the matrix $\mathcal{K}_p \in \mathbb{R}^{n_d \times pm_y}$ is defined as

$$\mathcal{K}_p \doteq [\, \widetilde{A}^{p-1}\widetilde{K} \quad \dots \quad \widetilde{A}\widetilde{K} \quad \widetilde{K}\,]. \tag{8}$$

Here, it should be noted that the ordering of the output data in the vector of past observations $y_p(k-p)$ differs form the one used in [19]. While in the previous definition all observations are ordered forward in time, the vector of past observations in the original presentation of SSARX is ordered backward in time. This will appear to be advantageous in achieving an efficient implementation. Furthermore, by using (6), the past and future outputs can be related as

$$y_f(k) = \mathcal{O}_f x(k) + \mathcal{T}_f y_f(k) + v_f(k) \tag{9}$$

where the extended observability matrix $\mathcal{O}_f$ and Toeplitz matrix of Markov parameters $\mathcal{T}_f$ are defined as

$$\mathcal{O}_f \doteq \begin{bmatrix} \widetilde{C} \\ \widetilde{C}\widetilde{A} \\ \vdots \\ \widetilde{C}\widetilde{A}^{f-1} \end{bmatrix} \quad \mathcal{T}_f \doteq \begin{bmatrix} 0 & \dots & 0 & 0 \\ \widetilde{C}\widetilde{K} & \ddots & & 0 \\ \vdots & \ddots & \ddots & \vdots \\ \widetilde{C}\widetilde{A}^{f-2}\widetilde{K} & \dots & \widetilde{C}\widetilde{K} & 0 \end{bmatrix}. \tag{10}$$

Consider the state estimate in (7) and the relation between past and future outputs (9), then the SSARX algorithm consists of the following steps. In the first step, a high-order AR model is estimated from the data to get an unstructured estimate of the Markov parameters $\widetilde{C}\widetilde{A}^i\widetilde{K}$ for $i \in \{0, \dots, f-2\}$. The estimated Markov parameters are then used to construct an estimate $\widehat{\mathcal{T}}_f$ of $\mathcal{T}_f$. In the next step, the estimate $\widehat{\mathcal{T}}_f$ is used to define the signal $z(k) \doteq (I - \widehat{\mathcal{T}}_f)y_f(k)$. Together with the definition $\mathcal{B} \doteq \mathcal{O}_f\mathcal{K}_p$, the approximation of $z(k)$ obtained by substituting (7) in (9) can be expressed as

$$z(k) \approx \mathcal{B}y_p(k-p) + v_f(k). \tag{11}$$

This equation can be viewed as a low rank linear regression problem in $\mathcal{B}$ and is used to obtain an estimate of $\mathcal{K}_p$. The least squares estimate of $\mathcal{B}$, in the sense that it minimizes the conditional expectation of the mean-square error between $z(t)$ and $\mathcal{B}y_p(k-p)$, is given by $\Gamma_{zp}(\Gamma_{pp})^{-1}$, where Γ_{zp} is the cross-correlation matrix between $z(k)$ and $y_p(k-p)$ and Γ_{pp} is the correlation matrix of $y_p(k-p)$. Given only a finite data set, the correlation matrices are approximated by their finite sample estimates $\widehat{\Gamma}_{zp}$ and $\widehat{\Gamma}_{pp}$, with

$$\widehat{\Gamma}_{zp} \doteq \frac{1}{N}\sum_{k=0}^{N-1} z(k)y_p^T(k-p) \tag{12}$$

and $\widehat{\Gamma}_{pp}$ defined accordingly. This gives rise to the following approximation $\widehat{\mathcal{B}} = \widehat{\Gamma}_{zp}\widehat{\Gamma}_{pp}^{-1}$ of $\mathcal{B}$. An estimate of the row space of $\mathcal{K}_p$ can now be obtained by factorizing $\widehat{\mathcal{B}}$. This is achieved by computing the SVD

$$M \doteq W_1\widehat{\mathcal{B}}W_2 = \widetilde{U}\widetilde{\Sigma}\widetilde{V}^T \tag{13}$$

where $\widetilde{U}$ and $\widetilde{V}^T$ are orthonormal matrices, $\widetilde{\Sigma}$ is a diagonal matrix composed of the singular values arranged in nondecreasing order, and W_1 and W_2 are nonsingular weighting matrices. The estimate of $\mathcal{K}_p$, up to a similarity transformation T, is then given by $\widehat{\mathcal{K}}_p = V_{n_d}^T W_2^{-1}$, where $V_{n_d}^T$ is the matrix composed of the first n_d columns of $\widetilde{V}^T$. In SSARX the row-space of $\mathcal{K}_p$ is estimated by performing a canonical correlation analysis (CCA) on the signals $z(k)$ and $y_f(k-p)$. This is equivalent to choosing the weighting matrices as $W_1 = \widehat{\Gamma}_{zz}^{-1/2}$ and $W_2 = \widehat{\Gamma}_{pp}^{1/2}$. These weighting matrices have the nice statistical property that they lead to the maximum likelihood estimate for a Gaussian linear regression problem with a rank constraint on the coefficient matrix [23]. The next step of SSARX consists of substituting the estimate of $\mathcal{K}_p$ in (7) to obtain an estimate of the corresponding state sequence $x(k)$. By replacing the true state with the estimate $\hat{x}(k) = V_{n_d}^T W_2^{-1} y_p(k-p)$, the system matrices can now be estimated by finite linear regression in the state space (6). Here the term finite linear regression refers to the linear regression problem obtained by replacing the conditional expectation by finite sample estimates, as was done to obtain $\widehat{\mathcal{B}}$. In this way, an estimate of the system matrices $\tilde{A}$ and $\tilde{K}$ is obtained by regressing $\hat{x}(k+1)$ on $\hat{x}(k)$ and $y(k)$. Likewise, the system matrix $\widetilde{C}$ is estimated by regressing $y(k)$ on $\hat{x}(k)$.

To arrive at an efficient implementation of the proposed algorithm, the data equations are expressed in terms of block Hankel matrices. Given N samples of the vector of past or future outputs $y_q(k), q \in \{p, f\}$, $Y_{i,q,N}$ is defined as

$$Y_{i,q,N} \doteq [\, y_q(i) \quad y_q(i+1) \quad \cdots \quad y_q(i+N-1)\,]$$

where the first entry of the subscript refers to the time index of its top left element, the second refers to the number of block rows, and the third refers to the number of columns. Using the same notational convention, the block Hankel matrix constructed from the vector of future innovations $v_f(k)$ will be denoted by $V_{i,f,N}$. By stacking time-shifted versions of (9), the equivalent data equation can be expressed as

$$(I - \widehat{\mathcal{T}}_f)Y_{p,f,N} \approx \mathcal{B}Y_{0,p,N} + V_{0,f,N}. \tag{14}$$

Recall that the first step in the SSARX algorithm is to identify a high-order AR model to get an unstructured estimate of the Markov parameters $\widetilde{C}\widetilde{A}^i\widetilde{K}i \in \{0,\ldots,f-1\}$. An important observation is therefore that (14) is nothing but the stacked outputs of an AR model. This implies that if the AR model order is not too high, the problem of identifying the Markov parameters can be conveniently expressed in terms of the block Hankel matrices in the above equation. By selecting the right block rows, the block Hankel matrices in (14) contain sufficient information for identifying an AR model of order $p+f-1$. However, since exploratory experiments show that for the considered type of data the choice of the AR model order has no or little influence on the overall performance, it will be chosen as small as possible for efficiency reasons. The order of the AR model will therefore be chosen $f-1$, which is the minimal amount needed to construct $\widehat{\mathcal{T}}_f$. The problem of identifying the AR coefficients can hence be formulated as

$$\min_{\widetilde{C}\mathcal{K}_{f-1}} ||Y_{p+f-1,1,N} - (\widetilde{C}\mathcal{K}_{f-1})Y_{p,f-1,N}||_F^2 \tag{15}$$

where $\|\cdot\|_F$ denotes the Frobenius norm and where, in accordance with (8), the matrix $\widetilde{C}\mathcal{K}_{f-1}$ is composed of the first $f-1$ Markov parameters. The coefficient matrix $\widetilde{C}\mathcal{K}_{f-1}$ that solves the previous optimization is known to be given by

$$\widehat{\widetilde{C}\mathcal{K}}_{f-1} = Y_{p+f-1,1,N}(Y_{p,f-1,N})^\dagger \tag{16}$$

where $(\cdot)^\dagger$ denotes the pseudo-inverse. Since the matrices $Y_{p+f-1,1,N}$ and $Y_{p,f-1,N}$ correspond to the last and first $f-1$ block rows of $Y_{p,f,N}$, respectively, the problem of identifying the Markov parameters can be completely expressed in terms of the data block Hankel matrices in (14).

Also, the problem of determining an estimate of $\mathcal{K}_p$ can be conveniently formulated in terms of the data block Hankel matrices. By comparing the definitions of the block Hankel and in (12), it is clear that the finite sample estimate of the correlation matrices Γ_{zp} and Γ_{pp} can be expressed as

$$\widehat{\Gamma}_{zp} = \frac{1}{N}(I - \widehat{\mathcal{T}}_f)Y_{p,f,N}Y_{0,p,N}^T \tag{17a}$$

$$\widehat{\Gamma}_{pp} = \frac{1}{N}Y_{0,p,N}Y_{0,p,N}^T. \tag{17b}$$

With the correlation matrix $\widehat{\Gamma}_{zz}$ expressed in a similar way, the previous equations could be used to compute the matrix $M \doteq W_1\widehat{\mathcal{B}}W_2$ for CCA weights W_1 and W_2 defined before. Instead of proceeding in this way, the proposed SSAR algorithm uses a different set of weights. More specifically, the weighting matrices are chosen as $W_1 = I$ and $W_2 = ((1/N)\Gamma_{pp})^{1/2}$, which corresponds to the weighting scheme used by the MOESP class of subspace algorithms [24]. This choice is motivated by the desire to reduce the computational complexity. Even though the CCA weighting scheme might be more attractive from a statistical point of view, it involves the additional step of computing the inverse square root of the estimated correlation matrix $\widehat{\Gamma}_{zz}$. For the MOESP weighting scheme, explicit computation of square root matrices can be avoided by using a square root implementation based on a single RQ factorization of the block Hankel matrices. This will be made more explicit in Theorem 1. Considering the new weights, the matrix M as defined in (13) becomes equal to $M = \sqrt{N}(\widehat{\Gamma}_{zp})(\widehat{\Gamma}_{pp})^{-1/2}$. By substituting the finite sample estimates (17a) and (17b), this gives rise to

$$M = (I - \widehat{\mathcal{T}}_f)Y_{p,f,N}Y_{0,p,N}^T\left(Y_{0,p,N}Y_{0,p,N}^T\right)^{-1/2}. \tag{18}$$

The corresponding estimate of the extended controllability matrix, $\widehat{\mathcal{K}}_p = \sqrt{N}V_{n_d}^T\widehat{\Gamma}_{pp}^{-1/2}$, can be expressed as

$$\widehat{\mathcal{K}}_p = V_{n_d}^T\left(Y_{0,p,N}Y_{0,p,N}^T\right)^{-1/2}. \tag{19}$$

Given the estimate of the extended controllability matrix $\mathcal{K}_p$, the remaining steps of proposed subspace identification algorithm are to reconstruct the approximate state sequence $\hat{x}(k) = V_{n_d}^T W_2^{-1} y_p(k-p)$, from which the system matrices are estimated by finite linear regression in the state-space equations. By selecting the right block-rows, also the finite linear regression step can be conveniently expressed in terms of the data block Hankel matrices $Y_{0,p,N}$ and $Y_{p,f,N}$. Using the same notational convention as for the data block Hankel matrices, the sequence of reconstructed states can be expressed as $\widehat{X}_{p,1,N} = \widehat{\mathcal{K}}_p Y_{0,p,N}$. Likewise, the sequence of time-shifted states is given by $\widehat{X}_{p+1,1,N} = \widehat{\mathcal{K}}_p Y_{1,p+1,N}$. From (6), it is clear that the finite linear regression problem used to estimate the system matrices $\widetilde{A}$ and $\widetilde{K}$ from the reconstructed state sequences $\widehat{X}_{p,1,N}$ and $\widehat{X}_{p+1,1,N}$, can formulated as

$$\min_{[\widetilde{A}|\widetilde{K}]} \left\| \widehat{X}_{p+1,1,N} - [\widetilde{A}|\widetilde{K}] \begin{bmatrix} \widehat{X}_{p,1,N} \\ Y_{p,1,N} \end{bmatrix} \right\|_F^2. \tag{20}$$

In the same way, the estimate of the system matrix $\widetilde{C}$ obtained by regressing $y_p(k-p)$ on $\hat{x}(k)$ can be expressed as the minimizing argument of the least squares optimization problem

$$\min_{\widetilde{C}} ||Y_{p,1,N} - \widetilde{C}\widehat{X}_{p,1,N}||_F^2. \tag{21}$$

The previous least squares optimization problems and reconstructed state sequences $\widehat{X}_{p,1,N}$ and $\widehat{X}_{p+1,1,N}$, give rise to the following estimate of the system matrices $\widetilde{A}$, $\widetilde{C}$, and $\widetilde{K}$

$$\widehat{[\widetilde{A}|\widetilde{K}]} = \widehat{\mathcal{K}}_p Y_{1,p+1,N}\begin{bmatrix} \widehat{\mathcal{K}}_p Y_{0,p,N} \\ Y_{p,1,N} \end{bmatrix}^\dagger \tag{22}$$

$$\widehat{\widetilde{C}} = Y_{p,1,N}(\widehat{\mathcal{K}}_p Y_{0,p,N})^\dagger. \tag{23}$$

The obtained estimate of the triple $(\widetilde{A},\widetilde{C},\widetilde{K})$ and the singular values Σ_1 of the geometry matrix, specify the system matrices of atmospheric disturbance model $\mathcal{S}$. By applying the definitions of $\widetilde{A}$, $\widetilde{C}$, and $\widetilde{K}$ it is possible to explicitly compute A_d, C_d, and K_d. As will be demonstrated in Section IV, this last step is not always necessary for computing the controller.

The different steps of the subspace algorithm have all been expressed in terms of the data block Hankel matrices $Y_{0,p,N}$ and $Y_{p,1,N}$. Even though these expressions provide a way to estimate $\widetilde{A}$, $\widetilde{C}$, and $\widetilde{K}$, this is computationally not attractive since the number of columns in the data block Hankel matrices is typically very large. However, due to specific choice of W_1 and W_2, the solution to each of the subproblems can be computed from the lower triangular (R) factor of the stacked data block Hankel matrix $Y_{0,p+f,N}$. Since the approach avoids the explicit computation of the square root matrices in (18) it will also improve the numerical robustness. The precise relation between each of the steps of the subspace algorithm and the R factor of the data block Hankel matrix is summarized in Theorem 1. The use of a RQ factorization to improve the computational efficiently of subspace algorithms is by no means new and has been proposed before in [24].

Theorem 1 (SSAR Via RQ Factorization): Given a signal $y(k) \in \mathbb{R}^{m_y}$, consider the economy size RQ factorization of the block Hankel matrix $Y_{0,p+f,N} \in \mathbb{R}^{(p+f)m_y \times N}$

$$\begin{bmatrix} Y_{0,1,N} \\ Y_{1,p-1,N} \\ Y_{p,1,N} \\ Y_{p+1,f-2,N} \\ Y_{p+f-1,1,N} \end{bmatrix} = \begin{bmatrix} R_{11} & 0 & 0 & 0 \\ R_{21} & R_{22} & 0 & 0 \\ \vdots & \vdots & \ddots & 0 \\ R_{51} & R_{52} & \cdots & R_{55} \end{bmatrix} \begin{bmatrix} Q_1 \\ Q_2 \\ \vdots \\ Q_5 \end{bmatrix} \quad (24)$$

where the R and Q factor are partitioned in accordance with the partitioning of the block-rows of $Y_{0,p+f,N}$ and $n_d \leq p\, m_y, f m_y \leq N$. Furthermore, let the matrices M and $\widehat{\mathcal{K}}_p$ be defined as in (18) and (19). Then the estimates in (16), (22), and (23), can be characterized in terms of the R factor only.

1) The solution to optimization problem (15) is given by

$$\widehat{\widetilde{C}\mathcal{K}}_{f-1} = [\, R_{51} \quad \cdots \quad R_{54}\,][\, R_{41} \quad \cdots \quad R_{44}\,]^{\dagger}.$$

2) Let $\widehat{\mathcal{T}}_f$ denote the matrix obtained by replacing $\widetilde{C}\widetilde{A}^i\widetilde{K}$ in (10) by the $f-i$th block column of the estimate $\widetilde{C}\mathcal{K}_{f-1}$, then

$$\widehat{M} = (I - \widehat{\mathcal{T}}_f) \begin{bmatrix} R_{31} & R_{32} \\ R_{41} & R_{42} \\ R_{51} & R_{52} \end{bmatrix} \quad \widehat{\mathcal{K}}_p = V_{n_d}^T \begin{bmatrix} R_{11} & 0 \\ R_{21} & R_{22} \end{bmatrix}^{\dagger}$$

where $V_{n_d}^T$ contains the right singular vectors corresponding to the n largest singular values of M.

3) Given $\widehat{\mathcal{K}}_p$ and $V_{n_d}^T$, the solutions to the optimization problems (20) and (21) can be expressed as

$$[\widehat{\widetilde{A}|\widetilde{K}}] = \widehat{\mathcal{K}}_p \begin{bmatrix} R_{21} & R_{22} & 0 \\ R_{31} & R_{32} & R_{33} \end{bmatrix} \left[\begin{array}{c|c} V_{nd}^T & 0 \\ \hline R_{31}\ R_{32} & R_{33} \end{array}\right]$$

$$\widehat{\widetilde{C}} = [\, R_{31} \quad R_{32}\,](V_{n_d}^T)^{\dagger}.$$

Proof: To proof the first statement, note that $Y_{p+1,f-3,N}$ and $Y_{p+f-2,1,N}$ can be expressed in terms of the submatrices of (24). Substituting these expressions in (16) and using the orthonormality of the Q-factor gives the desired result.

The second and third statement can be proved in a similar way. The matrices $Y_{0,p,N}$ and $Y_{p,p+f,N}$ are expressed in terms of the submatrices of RQ factorization (24) and the resulting expressions are substituted in (18) and (19). Using the orthogonality of the Q-factor leads to the given expressions for $\widehat{M}$ and $\widehat{\mathcal{K}}_p$. The condition $n \leq p\, m_y, f m_y \leq N$ guarantees that $\widehat{M}$ has at least n_d right singular vectors.

In proving the third statement, $Y_{0,p,N}$, $Y_{1,p+1,N}$, and $Y_{1,p+1,N}$ are expressed in terms of the RQ factor and the result is substituted in (22) and (23). Again, due to the orthogonality the Q-factor drops out. Substituting the expression for $\widehat{\mathcal{K}}_p$ in the pseudo-inverse term finally finishes the proof. ■

The previous theorem shows that the entire SSAR algorithm can be characterized in terms of the R factor of the block Hankel matrix $Y_{0,p+f,N}$ and that there is no need to actually compute Q. Since the computation of R is the only operation performed directly on the data block Hankel matrices, it has a large influence on the overall computational efficiency of the algorithm. To arrive at an efficient implementation, the R factor is computed by using the fast algorithm described by Mastronardi *et al.* [25]. Especially for large matrices, this algorithm is far more efficient than a standard RQ decomposition based on Householder transformations, as it is able to exploit the block Hankel structure in $Y_{0,p+f,N}$.

The choice of the user defined parameters f and p is a difficult issue in subspace identification [26]. In the SSARX algorithm, it is assumed that f and p are always chosen strictly larger than the system order n_d. With the stochastic disturbance model (4) being a minimal representation of the stochastic process, this is a sufficient condition to ensure that the matrix $\mathcal{B} = \mathcal{O}_f\mathcal{K}_p$ has rank n_d and can be factorized to find an estimate of the extended controllability matrix $\mathcal{K}_p$. For multivariable systems, the requirement $f, p > n_d$ may be overly conservative. As will be demonstrated by the numerical validation experiments in Section V, it may be useful to choose f and p much smaller than n_d. The parameters should, however, be chosen sufficiently large to guarantee that the rank of the matrix $\mathcal{B}$ is larger than the order of the identified disturbance model. A thorough consistency analysis of both the SSARX and the proposed algorithm is still a topic for future research.

IV. Computing the Optimal Controller

Given the WFS model (2), the DM model (3) and the atmospheric disturbance model (4), this section considers how to compute the controller that minimizes cost function (5). To this end, the AO control problem will be first formulated in a $\mathcal{H}_2$-framework. Even though this approach is very general, it is unable to exploit the structure in the AO problem. Computing the $\mathcal{H}_2$-optimal controller generally involves the need to solve two Riccati equations. By transforming the AO control problem in an equivalent feedforward problem, it will be shown that due to the minimum-phase property of the disturbance model at least one of the Riccati equations can be avoided. Furthermore, it will be shown that if the DM and WFS dynamics can be modeled as a delay and a two taps impulse response, an analytical expression can be derived. This is attractive from both the viewpoint of computational efficiency and numerical robustness. Since the poles of the atmospheric disturbance model typically cluster in the neighborhood of the point $z = -1$, standard

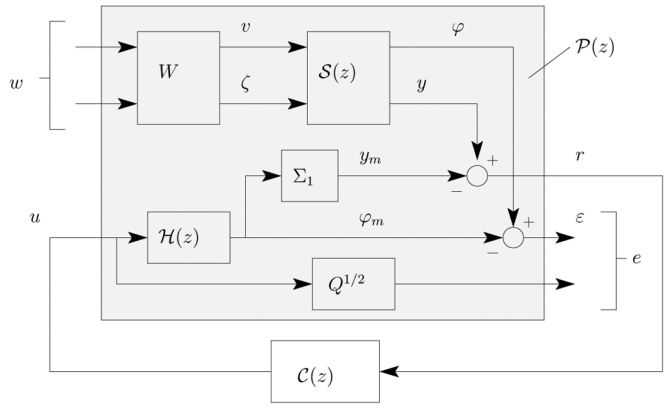

Fig. 4. Block-diagram of AO system in generalized plant representation.

Riccati solvers [27] may suffer from convergence problems and increased numerical sensitivity. Moreover, the analytical solution provides more insight in the relation with the common AO control approach.

Consider Fig. 4, which provides a schematic representation of the AO control problem in the so-called generalized plant framework. The generalized plant $\mathcal{P}(z)$, indicated by the shaded block, is assumed to have a zero-mean white noise disturbance input $w(k)$ with unit covariance $\mathcal{E}\{w(k)w^T(k)\} = I$. The exogenous disturbance inputs $v(k)$ and $\zeta(k)$ to the atmospheric disturbance model $\mathcal{S}(z)$, however, are zero-mean and white, but are not uncorrelated and do not have unit covariance. To fit the AO control problem in the generalized plant framework, the atmospheric disturbance model $\mathcal{S}(z)$ is preceded by the static input weight W, which generates the signals $v(k)$ and $\zeta(k)$ with the proper covariance and cross-covariance matrices out of $w(k)$. The input weight W should hence be equal to the square root covariance matrix of the signal obtained by stacking $v(k)$ and $\zeta(k)$. To compute this weight W, note that the measurement noise $n(k)$ should be uncorrelated with the wavefront distortions $\varphi(k)$ and the state vector $x(k)$. By multiplying the second output equation in (4) from the right by $n^T(k)$ and substituting the definition of $\zeta(k)$, we can, therefore, write

$$\begin{aligned}\mathcal{E}\left\{\varphi(k)n^T(k)\right\} &= \mathcal{E}\left\{\left(C_d x(k) - \Sigma_1^{-1}\zeta(k)\right)n^T(k)\right\} = 0\\ &= \Sigma_1^{-1}(R_{vn} - R_n)\end{aligned}$$

where $R_{vn} \doteq \mathcal{E}\{v(k)n^T(k)\}$ and $R_n \doteq \mathcal{E}\{n(k)n^T(k)\}$. From the above equation we infer that $R_{vn} = R_n$, which gives rise to the following cross-covariance matrix

$$\begin{aligned}R_{v\zeta} &= \mathcal{E}\left\{v(k)\left(\left(v^T(k) - n^T(k)\right)\Sigma_1^{-1}\right)\right\}\\ &= \left(R_v - R_n\right)\Sigma_1^{-1}.\end{aligned}$$

In the same way, the covariance matrix R_ζ can be expressed as $R_\zeta = \Sigma_1^{-1}(R_v - R_n)\Sigma_1^{-1}$. From these expressions, we infer that the weighting matrix W can be chosen as

$$W = \mathcal{E}\left(\begin{bmatrix}v(k)\\ \zeta(k)\end{bmatrix}[\cdot]^T\right)^{1/2} = \begin{bmatrix}R_v^{1/2} & 0\\ \Xi_1 & \Xi_2\end{bmatrix} \qquad (25)$$

where

$$\Xi_1 \doteq \Sigma^{-1}\left(R_v^{1/2} - R_n R_v^{-1/2}\right)$$

and

$$\Xi_2 \doteq \Sigma_1^{-1}\left(R_n - R_n R_v^{-1} R_n\right)^{1/2}.$$

Note that since $\mathcal{S}(z)$ is assumed to be minimal and R_n is nonsingular, W has full rank and defines a bijective mapping. Furthermore, because W is upper triangular, the weighting preserves the minimum-phase property of $\mathcal{S}(z)$.

As depicted in Fig. 4, the performance output of the generalized plant $\mathcal{P}(z)$ is defined as $e(k) = [\varepsilon^T(k) \quad u^T(k)Q^{T/2}]^T$. For this choice, the MSE of $e(k)$ is equal to cost function (5). Let $\mathcal{P}(z)$ be partitioned in accordance with the partitioning of the input and output signals, and let the corresponding transfer functions be denoted by $\mathcal{P}_{ew}(z)$, $\mathcal{P}_{eu}(z)$, $\mathcal{P}_{rw}(z)$, and $\mathcal{P}_{ru}(z)$. Then by Parseval's theorem, the MSE of $e(k)$ is equal to the $\mathcal{H}_2$-norm of the closed loop transfer function

$$\mathcal{F}(\mathcal{P},\mathcal{C}) = \mathcal{P}_{ew} + \mathcal{P}_{eu}(I - \mathcal{C}\mathcal{P}_{ru})^{-1}\mathcal{C}\mathcal{P}_{rw}.$$

This implies that the AO control problem reduces the standard $\mathcal{H}_2$-optimal problem of finding the controller $\mathcal{C}(z)$ that minimizes the $\mathcal{H}_2$-norm of $\mathcal{F}(\mathcal{P},\mathcal{C})$. By combining the models of the WFS, the DM, the atmospheric disturbance model, and the input weighting, the $\mathcal{P}(z)$ can be expressed as

$$\left[\begin{array}{c}\xi(k+1)\\ \hline e(k)\\ \hline r(k)\end{array}\right] = \left[\begin{array}{cc|cc|c}A_m & 0 & 0 & 0 & B_m\\ 0 & A_d & K_d R_v^{1/2} & 0 & 0\\ \hline -C_m & C_d & \Xi_1 & \Xi_2 & 0\\ 0 & 0 & 0 & 0 & Q^{1/2}\\ \hline -\Sigma_1 C_m & \Sigma_1 C_d & R_v^{1/2} & 0 & 0\end{array}\right]\left[\begin{array}{c}\xi(k)\\ \hline w(k)\\ \hline u(k)\end{array}\right].$$

From the previous discussion, it is clear that the AO control problem can be solved by applying standard $\mathcal{H}_2$-optimal control theory (see [28] and [29]) to the previous state-space realization.

In order to exploit the structure in the AO control problem, however, a different strategy will be used. To this end, the AO control problem is transformed to an equivalent feedforward problem, which is then solved by using causal Wiener filtering. This strategy is known as the internal model control (IMC) approach [30]. Since the WFS and DM mirror models are assumed to be known, the open-loop wavefront signal $y(k)$ can be reconstructed by subtracting the influence of the DM on the measured WFS signal $r(k)$, i.e., $y(k) = r(k) - \Sigma_1\mathcal{H}(z)u(k)$. In this way, it is possible to open the feedback loop and replace the original control problem by that of finding the optimal feedforward controller $u(k) = \mathcal{W}(z)y(k)$. Fig. 5 provides a block-diagram of the equivalent feedforward problem. As can be easily verified,

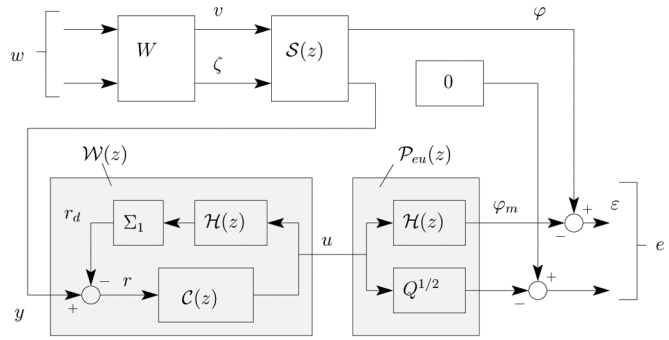

Fig. 5. Block-scheme of equivalent feedforward AO control system.

the feedforward controller $\mathcal{W}(z)$ and feedback controller $\mathcal{C}(z)$ are related in the following way

$$\mathcal{C}(z) = \mathcal{W}(z)(I - \Sigma_1 \mathcal{H}(z)\mathcal{W}(z))^{-1}. \tag{26}$$

For stable $\mathcal{H}(z)$, the class of stable $\mathcal{W}(z)$ parametrizes all stabilizing closed-loop controllers $\mathcal{C}(z)$. This parameterization is the so-called Youla parameterization [31]. Considering the performance output $e(k)$ of $\mathcal{P}(z)$, it follows from the Parseval theorem that the relation between the cost function (5) and the $\mathcal{H}_2$-norm of the open-loop transfer function is given by

$$J = \|\mathcal{P}_{ew} - \mathcal{P}_{eu}\mathcal{W}\mathcal{P}_{yw}\|_2^2 \tag{27}$$

where $\mathcal{P}_{yw}$ denotes the open-loop transfer function from $w(k)$ to $y(k)$. Given the transfer functions $\mathcal{P}_{eu}(z)$, $\mathcal{P}_{ew}(z)$, and $\mathcal{P}_{yw}(z)$, the solution to the problem of finding the optimal feedforward controller $\mathcal{W}(z)$ that minimizes J is given by the causal Wiener filter summarized in Lemma 1. If $I + \mathcal{P}_{eu}(z)\mathcal{W}(z)$ is invertible, the optimal feedback controller $\mathcal{C}(z)$ can be computed from the Youla parameterization (26).

Lemma 1 (Causal Wiener Filter [32]): Let $\mathcal{P}_{ew}$, $\mathcal{P}_{eu}$ and $\mathcal{P}_{yw}$ be strictly stable rational transfer functions, and assume that $\mathcal{P}_{eu}(z)$ and $\mathcal{P}_{yw}(z)$ do not loose rank $\forall|z| = 1$. Then the feedforward controller that minimizes (27) is given by

$$\mathcal{W} = -\mathcal{P}_{eu,o}^{\dagger}\left[\mathcal{P}_{eu,i}^{*}\mathcal{P}_{ew}\mathcal{P}_{yw,i}^{*}\right]_{+}\mathcal{P}_{yw,o}^{\dagger} \tag{28}$$

with $[\cdot]_+$ the causality operator, $\mathcal{P}_{eu} = \mathcal{P}_{eu,i}\mathcal{P}_{eu,o}$ the inner-outer factorization of $\mathcal{P}_{eu}$, $\mathcal{P}_{yw} = \mathcal{P}_{yw,o}\mathcal{P}_{yw,i}$ the outer-inner factorization of $\mathcal{P}_{yw}$, and $(\cdot)^{\dagger}$ the pseudo inverse. Here $\mathcal{P}_{eu} = \mathcal{P}_{eu,i}\mathcal{P}_{eu,o}$ is an inner-outer factorization of $\mathcal{P}_{eu}$ if $\mathcal{P}_{eu,i}$ and $\mathcal{P}_{eu,o}$ are strictly stable, $\mathcal{P}_{eu,i}^{*}\mathcal{P}_{eu,i} = I$ and $\mathcal{P}_{eu,o}$ has a stable right inverse. Likewise, $\mathcal{P}_{yw} = \mathcal{P}_{yw,o}\mathcal{P}_{yw,i}$ is an outer-inner factorization of $\mathcal{P}_{yw}$ if $\mathcal{P}_{yw,o}$ and $\mathcal{P}_{yw,i}$ are strictly stable, $\mathcal{P}_{yw,i}\mathcal{P}_{yw,i}^{*} = I$ and $\mathcal{P}_{eu,o}$ has a stable left inverse.

As demonstrated in [32], the inner-outer and outer-inner factorizations of $\mathcal{P}_{eu}(z)$ and $\mathcal{P}_{yw}(z)$ can be both expressed in terms of the solution of a Riccati equation. This implies that also the approach of computing the optimal feedback controller via Wiener filtering generally involves the need to solve two Riccati equations. More specifically, the Riccati equation encountered in computing the outer-inner factorization of $\mathcal{P}_{yw}$ is equal to the one encountered in determining the state observer in the LQG or $\mathcal{H}_2$-optimal control setting. The Riccati equation encountered in computing the inner-outer factorization of $\mathcal{P}_{eu}(z)$, on the other hand, can be associated with computing the state-feedback gain. Due to the special structure of the atmospheric disturbance model, however, it is possible to directly give a valid outer-inner factorization of $\mathcal{P}_{yw}(z)$. The state-space realization of $\mathcal{P}_{yw}(z)$ is given by

$$\mathcal{P}_{yw}(z) = \left[\left(\Sigma_1 C_d(zI - A_d)^{-1}K_d + I\right)R_v^{1/2} \quad 0\right]. \tag{29}$$

Since the atmospheric disturbance model is in innovation form and $R_v^{1/2}$ is nonsingular, $\mathcal{P}_{yw}$ is minimum-phase. This implies that the outer factor can be chosen equal to the transfer function itself, i.e., $\mathcal{P}_{yw} = \mathcal{P}_{yw,o}$. As a result, the outer-inner factorization of $\mathcal{P}_{yw}(z)$ does not need to be computed and the corresponding Riccati equation drops out. Note that this can also be understood from a $\mathcal{H}_2$-optimal control perspective. Since the Kalman gain K_d is already known, no Riccati equation has to be solved to determine the state-observer.

Like $\mathcal{P}_{yw}(z)$, the state-space realization of $\mathcal{P}_{ew}(z)$ can be immediately read off from the atmospheric disturbance model (4) and the derived input weighting (25), i.e.,

$$\mathcal{P}_{ew}(z) = \begin{bmatrix} C_d(zI - A_d)^{-1}K_d R_v^{1/2} + \Xi_1 & \Xi_2 \\ 0 & 0 \end{bmatrix}.$$

Furthermore, it follows from the choice of the performance output $e(k)$ that $\mathcal{P}_{eu}(z) = [\mathcal{H}^T(z) \quad Q^{T/2}]^T$. The previous state-space realizations of $\mathcal{P}_{ew}$, $\mathcal{P}_{eu}$, and the outer-inner factorization of $\mathcal{P}_{yw}$ can be used to compute the optimal controller $\mathcal{C}(z)$. Instead of considering the general DM mirror (3), it is interesting to focus on the case where the DM can be considered as approximately static. Since the bandwidth of the DM is usually much larger than the control bandwidth [14], this is a reasonable assumption for a large class of AO systems. When the DM settling time can be neglected with respect to the WFS exposure-time, the dynamics of transfer function from $u(k)$ to $y(k)$ are completely determined by the zero-order hold (ZOH) nature of the digital-to-analog conversion, the integrating action related to the finite exposure-time of the WFS and the time delay caused by data acquisition and processing. With the WFS exposure-time being smaller than the sampling time T, this implies that the DM, including the WFS dynamics $g(z)$, can be modeled as

$$\mathcal{H}(z) = z^{-d}\left(H + \alpha z^{-1}H\right) \tag{30}$$

where $\alpha \in \mathbb{R}$, $d \in \mathbb{N}$ denotes the number of samples pure delay, and $H \in \mathbb{R}^{m_p \times m_u}$ the DM influence matrix. Since there is a finite delay between measurement and correction, the condition $d \geq 1$ should always be satisfied.

Considering the previous DM model structure, it is possible to derive an analytical expression for the optimal controller $\mathcal{C}(z)$. To this end, note that since $\mathcal{P}$ is time-invariant each of the channels of $e(k)$ can be delayed by an integer number of samples without modifying the cost function. By introducing a d-samples delay in the channels that correspond to the control effort, i.e., $\mathcal{P}_{eu}(z) = [\mathcal{H}^T(z) \quad z^{-d}Q^{T/2}]^T$, all channels of $\mathcal{P}_{eu}(z)$ are delayed by the same amount so that the delay z^{-d} can be factored out. As can be easily verified, this gives rise to a valid inner-outer factorization of $\mathcal{P}_{eu}(z)$ for $|\alpha| \leq 1$. A similar

strategy can be followed for $|\alpha| > 1$. Since the cost function is not influenced by an all-pass filter, the all-pass filter that contains the non-minimum-phase zero of $\mathcal{H}(z)$ can be factored out. This leads to the following factorization:

$$\mathcal{P}_{eu}(z) = \begin{cases} \frac{1}{z^d} I \times \begin{bmatrix} -(1+\alpha z^{-1})H \\ Q^{1/2} \end{bmatrix}, & \text{for } |\alpha| \leq 1 \\ \frac{(z+\alpha)}{z^d(\alpha z+1)} I \times \begin{bmatrix} -(\alpha+z^{-1})H \\ Q^{1/2} \end{bmatrix}, & \text{for } |\alpha| > 1. \end{cases}$$

The derived expressions for the inner-outer and outer-inner factorizations of $\mathcal{P}_{eu}(z)$ and $\mathcal{P}_{yw}(z)$, can be used to compute the optimal feedback controller via Lemma 1 and the Youla parameterization (26). This leads to the following theorem.

Theorem 2 (Optimal Control Quasi-Static DM): Let the signals $\varphi(k)$ and $y(k)$ be characterized by the regular stochastic process (4) with $R_v > 0$. Furthermore, assume that the DM (including the WFS dynamics) can be modeled as (30) and that either H or Q has full column rank (i.e., $[\,H^T \quad Q^{T/2}\,]^T$ is left invertible). Then the optimal feedforward controller $\mathcal{W}(z)$ that minimizes (5), is given by

$$\left[\begin{array}{c} \hat{\chi}_1(k+1) \\ \hat{\chi}_2(k+1) \\ \hline u(k) \end{array}\right] = \left[\begin{array}{cc|c} \widetilde{A} & 0 & K_d \\ F\widetilde{A} & -G & FK_d \\ \hline F\widetilde{A} & -G & FK_d \end{array}\right] \left[\begin{array}{c} \hat{\chi}_1(k) \\ \hat{\chi}_2(k) \\ \hline y(k) \end{array}\right] \quad (31)$$

where the matrices $\widetilde{A}$, F, and G are defined as $\widetilde{A} \doteq A_d - K_d\Sigma_1 C_d$, $F \doteq H_Q^\dagger C_d A^{d-1}$, and $G \doteq \gamma_\alpha H_Q^\dagger H$, and where

$$H_Q^\dagger \doteq \begin{cases} (H^T H + Q)^{-1} H^T, & \text{for } \alpha = 0 \\ \alpha\gamma_\alpha \left(\alpha^2 H^T H + \gamma_\alpha^2 Q\right)^{-1} H^T, & \text{otherwise} \end{cases} \quad (32)$$

with

$$\gamma_\alpha \doteq \begin{cases} \alpha, & \text{for } |\alpha| \leq 1 \\ \operatorname{sgn}(\alpha), & \text{for } |\alpha| > 1 \end{cases}$$

can be interpreted as a regularized left pseudo-inverse of the influence matrix H. Furthermore, let the matrices L and M be defined as $L \doteq z^{-d+1} K_d \Sigma_1 H(\alpha I - G)$ and $M \doteq \widetilde{A} + z^{-d+1} K_d \Sigma_1 H F$. Then the corresponding optimal feedback controller $\mathcal{C}(z)$ has a state-space representation which can be seen in the equation at the bottom of the page.

Theorem 2 provides an analytical solution to the AO optimal control problem in case the DM model and the WFS dynamics can be described by (30). Given the matrix Σ_1 composed of the nonzero singular values of G and the DM influence matrix H, Theorem 2 can be used to compute the optimal controller from the system matrices $\widetilde{A}$, $\widetilde{C}$, and $\widetilde{K}$. This in combination with the proposed subspace identification algorithm gives rise to a direct and noniterative way to go from open-loop measurement data to closed-loop controller design. The resulting closed-loop control design procedure is entirely based on standard matrix operations. Note that due to the presence of the $(d-1)$ samples delay in the state-update equations for ξ_2, the optimal feedforward and feedback controllers in Theorem 2 are effectively of order $n_d + m_u(d-1)$.

To obtain more insight in the structure of the analytical expressions of the optimal controller, it is useful to consider the case where the combined DM and WFS dynamics consists of a pure delay, i.e., $\mathcal{H}(z) = z^{-d}H$. Physically this situation can be achieved by accurate synchronization of the DM digital-to-analog converters and the WFS exposure time. When the DM settling time is negligible and the digital-to-analog converters are synchronized in such a way that the ZOH output does not change during the CCD exposure time, the only dynamics that are left is a pure delay. The expressions for the optimal controller in this case are immediately obtained from Theorem 2 and are summarized in Corollary 1.

Corollary 1 (Multiple-Sample Delay): Consider an AO system where the only dynamics exhibited by the WFS and DM is a number of samples delay, i.e., $\mathcal{H}(z) = z^{-d}H$. Furthermore assume that the conditions in Theorem 2 are satisfied, then the optimal feedforward controller $\mathcal{W}(z)$ is given by

$$\left[\begin{array}{c} \hat{\chi}_1(k+1) \\ \hline u(k) \end{array}\right] = \left[\begin{array}{c|c} \widetilde{A} & K_d \\ \hline F\widetilde{A} & FK_d \end{array}\right] \left[\begin{array}{c} \hat{\chi}_1(k) \\ \hline y(k) \end{array}\right]. \quad (33)$$

Furthermore, the optimal feedback $\mathcal{C}(z)$ that internally stabilizes $\mathcal{P}(z)$ has a state-space representation

$$\left[\begin{array}{c} \hat{\xi}_1(k+1) \\ \hline u(k) \end{array}\right] = \left[\begin{array}{c|c} \widetilde{A} + z^{-d+1} K_d \Sigma_1 H F & K_d \\ \hline F(\widetilde{A} + z^{-d+1} K_d \Sigma_1 H F) & FK_d \end{array}\right] \left[\begin{array}{c} \hat{\xi}_1(k) \\ \hline r(k) \end{array}\right]$$

where $\widetilde{A}$ and F are defined as in Theorem 2, and $H_Q^\dagger$ reduces to the expression $H_Q^\dagger = (H^T H + Q)^{-1} H^T$.

The state-space (33) for $\mathcal{W}(z)$ allow for a nice physical interpretation. To make this clear, consider the atmospheric disturbance model (4) and let $\hat{x}(k|k-1)$ denote the conditional mean of $x(k)$ given the past open-loop WFS data $\{y(j), j \leq k-1\}$. By using the output equation to eliminate $v(k)$, the conditional mean at the next sample can be expressed as $\hat{x}(k+1|k) =$

$$\left[\begin{array}{c} \hat{\xi}_1(k+1) \\ \hat{\xi}_2(k+1) \\ \hline u(k) \end{array}\right] = \left[\begin{array}{cc|c} -G & F & 0 \\ L & M & K_d \\ \hline FL+G^2 & FM-GF & FK_d \end{array}\right] \left[\begin{array}{c} \hat{\xi}_1(k) \\ \hat{\xi}_2(k) \\ \hline r(k) \end{array}\right]$$

$\widetilde{A}\hat{x}(k|k-1)+K_d y(k)$. From this, it is clear that the state in (33) can be interpreted as $\hat{x}(k|k-1)$. In fact, the state corresponds to the state in the Kalman predictor model. The unpredictability of the white noise $v(k)$ causes the optimal prediction of future states to be obtained by iterating (4) with $v(k)=0$ [33]. This gives rise to the state estimate $\hat{x}(k+d|k)=A^{d-1}\hat{x}(k+1|k)$. By comparing this with the output equation of $\mathcal{W}(z)$, it is clear that the control signal can be expressed as $u(k)=H_Q^{\dagger}C\hat{x}(k+d|k)$. With $\hat{x}(k+d|k)$ being the conditional mean of the state of the atmospheric disturbance model (4), $\hat{\varphi}(k+d|k)\doteq C\hat{x}(k+d|k)$ can be interpreted as the conditional mean of $\varphi(k+d)$ given the past open-loop WFS data $\{y(j), j\leq k\}$. On the other hand, $H_Q^{\dagger}$ can be seen as a regularized version of the pseudo-inverse of the DM influence matrix H and provides a projection of the estimated phase $\hat{\varphi}(k+d|k)$ on the DM actuator space. This demonstrates that the optimal feedforward controller $\mathcal{W}(z)$ decomposes in a multiple step ahead predictor, which is concerned with estimating the uncorrected wavefront $\varphi(k+d)$, and a static matrix projection. This can be well understood in the context of the feedforward control problem in Fig. 5. Since the feedforward and feedback control problems are equivalent through the Youla parameterization, the interpretation of the structure of the $\mathcal{W}(z)$ can be extended to the feedback case. For this reason, the state of the optimal feedback controller $\mathcal{C}(z)$ can be seen as the conditional mean $\hat{x}(k|k-1)$ given the closed-loop WFS measurements $r(j), j\leq k-1$.

The previous interpretation can be used to obtain more insight in the structure of the optimal controller in the more general case that the DM model and WFS dynamics are described by (30). To this end note that the first state-update equation in (31) and the state-update equation in (33) are equal. This implies that $\hat{\chi}_1(k)$ can still be interpreted as the conditional mean $\hat{x}(k|k-1)$ of the state $x(k)$. Furthermore, since the second state-update equation is equal to the output equation, it is clear that the state $\hat{\chi}_2(k+1)$ is equal to the control signal $u(k)$. Using the previous interpretations, the output $u(k)$ of the optimal controller in Theorem 2 can be expressed as

$$u(k)=H_Q^{\dagger}\hat{\varphi}(k+d|k)-\gamma_a H_Q^{\dagger}Hu(k-1) \tag{34a}$$

$$=\left(I-\gamma_a H_Q^{\dagger}Hz^{-1}\right)^{-1}H_Q^{\dagger}\hat{\varphi}(k+d|k). \tag{34b}$$

This shows that the optimal controller still consists of a part that is concerned with estimating $\hat{\varphi}(k+d|k)$ but that the static projection $H_Q^{\dagger}$ has been replaced by a dynamic filter. The dynamic filter makes a tradeoff between the problem of inverting the undelayed part of the DM model $(1+\alpha z^{-1})H$ and the problem of minimizing the control effort. This can be easily seen for the case that $|\alpha|<1$ and $Q=0$. For this specific case $\gamma_\alpha H_Q^{\dagger}H=\alpha I$, so that the dynamic filter reduces to $(1+\alpha z^{-1})^{-1}H^{\dagger}$, which is precisely the inverse of $(1+\alpha z^{-1})H$. Due to the equivalence between the feedforward and feedback control problem, also the output of $\mathcal{C}(z)$ can be expressed as in (34a), where the conditional mean $\hat{\varphi}(k+d|k)$ is now determined on the basis of the closed-loop WFS measurements $r(j), j\leq k-1$.

V. Simulation Results

The closed-loop control design approach obtained by combining the subspace algorithm and the analytical solution to the $\mathcal{H}_2$-optimal control problem, has been validated on the basis of open-loop WFS data obtained from an AO test bench.

In the simulation experiments, the performance of the proposed control strategy is compared with a control approach commonly used in AO. Before discussing the simulation experiments, the common AO control approach will be briefly summarized. For conformity with the rest of the paper, this discussion will be in terms of the reduced signals introduced in Section II.

The common AO control approach consists of the cascade of a static matrix multiplication and a series of parallel feedback loops [4]. Given a new WFS measurement $y(k)$, the static part is concerned with the problem of finding the DM actuator inputs $u(k)$ that would provide the best fit to the wavefront. In this step, the temporal dynamics of both the wavefront disturbance and the AO system are neglected. This is to say that DM is modeled as $\varphi_m(k)=Hu(k)$ while the WFS is described by the static WFS model obtained by setting $\mathcal{G}(z)=G$ in (1). Considering the static relation $u(k)=Ry(k)$, the problem of finding the matrix R that provides the best fit to the wavefront can now be formulated as

$$R=\arg\min_R \mathcal{E}\left\{\|\varphi(k)-HRy(k)\|_2^2\right\} \tag{35}$$

where $\|\cdot\|_2$ denotes the $\mathcal{L}_2$-norm and $\mathcal{E}$ is the conditional expectation given the WFS measurement $y(k)$. Let the covariance matrices of the measured wavefront $\varphi(k)$ and the measurement noise $n(k)$ be defined as $C_\varphi\doteq\mathcal{E}\{\varphi(k)\varphi^T(k)\}$ and $C_n\doteq\mathcal{E}\{n(k)n^T(k)\}$, respectively. Then, under the assumption that $n(k)$ and $\varphi(k)$ are uncorrelated and $C_n=\sigma_n^2 I$, the maximum *a posteriori* estimate of R is given by

$$R=(H^TH)^{-1}H^T\left(\Sigma_1^2+\sigma_n^2C_\varphi^{-1}\right)^{-1}\Sigma_1$$

where σ_n^2 denotes the measurement noise variance. The signal $u(k)$ computed from the reconstruction process cannot be used directly as the control signal. Since the AO system is operated in closed-loop, the WFS measures the residual wavefront $\varepsilon(k)=\varphi(k)-\varphi_m(k)$ instead of $\varphi(k)$. This implies that the signal obtained from the static reconstruction $u(k)=Rr(k)$ provides only an estimate of the correction that has to be applied to current actuator commands. The parallel feedback loops are responsible for stability and closed-loop performance and have to posses integrating action to overcome this shortcoming. In this paper, the following controller has been used for performance comparison:

$$u(k)=\frac{\beta}{1-\alpha z^{-1}}Rr(k) \tag{36}$$

where $\alpha\in\mathbb{R}$ and $\beta\in\mathbb{R}$ are user defined control parameters. As usual, the change in C_φ due to closed-loop operation is neglected in the common AO control approach.

The proposed data-driven $\mathcal{H}_2$-optimal control approach has been validated for the case that the DM and WFS are static up to a unit-sample delay, i.e., $\mathcal{H}(z)=z^{-1}H$. The open-loop WFS data used in the simulation experiments have been obtained from an AO test bench. The AO test bench uses a turbulence simulator consisting of a circular glass plate that is rotated

through the optical beam, emulating a single layer of frozen turbulence satisfying the Taylor hypothesis. One side of the glass plate has been machined to introduce wavefront distortions with a Kolmogorov like spatial distribution characterized by a D/r_0 of 5, where $D = 10$ mm is the diameter of the simulated telescope aperture and r_0 denotes the Fried parameter [2]. The glass plate is rotated with such a speed that the Greenwood frequency of the distortions is $f_G = 0.95$ Hz. Since the temporal error scales as $\sigma_T^2 \propto (f_G/f)^{5/3}$[2], the AO test bench has the same temporal error as an AO system with a sample frequency of $f = 296$ Hz and a Greenwood frequency of $f_G = 11.25$ Hz. The open-loop WFS data are recorded by using a Shack-Hartmann WFS with an orthogonal micro-lens array. After aligning the setup, 53 micro-lenses are illuminated sufficiently to be used for wavefront sensing. This gives rise to a WFS signal $s(k)$ of dimension $m_s = 106$. The geometry matrix G in the simulations was defined defined according to the Fried geometry. Considering this matrix, $y(k) = U_1^T s(k)$ has a dimension of $m_y = 69$. All simulations are performed on the basis of 10^4 samples collected at a sampling rate of 25 Hz. The collected data set is divided into two parts. The first $N_i = 8000$ samples are used to identify the atmospheric disturbance model, while the remaining $N_v = 2000$ samples are reserved for performance evaluation.

Two simulation scenarios have been elaborated. The first scenario consists of closed-loop simulations with an ideal DM. Here, the term ideal refers to a hypothetical case that the DM is able to take the shape of the estimated wavefront without introducing a fitting error. This means that the DM influence matrix H is assumed to have full row rank. The ideal DM should therefore have at least as many actuators as independent WFS channels, i.e., $m_u \geq m_y$. Even though this condition is hardly ever satisfied, it is interesting to consider as it provides a better insight in error sources other than the fitting error. Note that from the physical interpretation of the optimal controller in Section IV it is clear that in this case the residual phase error is equal to the wavefront prediction error, i.e., $\varepsilon(k) = \varphi(k) - \hat{\varphi}(k|k-1)$. The second simulation scenario considers a more realistic DM model. In this case, the DM model is obtained by identifying the influence matrix of the DM used in the test bench. This is a 37-actuator electrostatic membrane mirror (i.e., $m_u = 37$) provided by OKO technologies, The Netherlands. The mirror is operated around an offset and is linear with the applied voltage squared. The DM influence matrix H has been estimated from a least squares fit on the reconstructed wavefront data obtained by measuring the steady state WFS response y_m to a set of predefined inputs u. In the simulation experiments, the performance of the proposed control design strategy has been compared with the common AO control law in (36). The control parameters α and β have been tuned so as to optimize the cost function, which resulted in the values $\alpha = 1.31$ and $\beta = 0.997$. The covariance matrix C_φ has been computed by assuming a perfect Kolmogorov spatial distribution with a Fried parameter r_0 satisfying the specification of the turbulence simulator. The variance of the measurement noise σ_n^2 has been estimated by computing the variance of the WFS measurements $y(k)$ for a static wavefront distortion $\varphi(k)$ generated by the turbulence simulator.

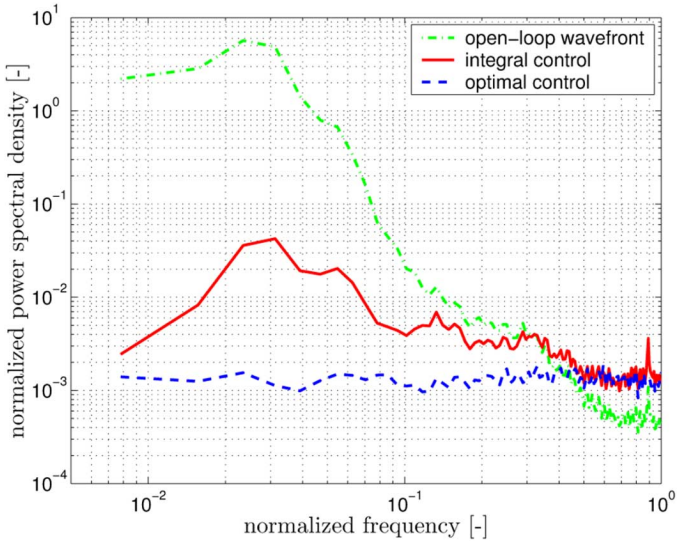

Fig. 6. Normalized averaged power spectrum $P(\omega)$ residual wavefront for closed-loop simulations with an ideal DM.

In testing the proposed control design strategy, the number of block-rows p and f used in the subspace identification step has been chosen equal to 15. These parameters are used to identify an atmospheric disturbance model of order $n_d = 300$. The control-effort weighting in cost function (5) is neglected in the simulations by choosing $Q = 0$.

In evaluating the performance of the controller, two different performance measures have been computed on the basis of the simulated residual phase error $\varepsilon(k)$ for $k \in \{1, \ldots, N_v\}$. The first performance measure can be interpreted as a normalized version of the mean-square residual error and is defined as

$$J_1 = \frac{\sum_{k=1}^{N_v} \mathrm{tr}(\varepsilon(k)\varepsilon^T(k))}{\sum_{k=1}^{N_v} \mathrm{tr}(\varphi(k)\varphi^T(k))}.$$

The performance index J_1 provides a quantitative measure of the total reduction in the mean-square residual phase error and is independent of the scaling of the wavefront. Furthermore, to obtain some more insight in the temporal dynamics of the controller it is useful to consider the normalized averaged power spectrum $P(\omega)$ of the residual phase error

$$P(\omega) = \frac{\sum_{j=1}^{m_y} \Phi_j(\omega)}{\frac{1}{N_v}\sum_{k=1}^{N_v} \mathrm{tr}(\varphi(k)\varphi^T(k))}$$

where $\Phi_j(\omega)$ is the estimated power spectral density of the jth component of the residual wavefront $\varepsilon(k)$, evaluated at ω. $\Phi_j(\omega)$ is computed as the Welch averaged periodogram with a window size of 256.

Figs. 6 and 7 show the normalized averaged power spectra $P(\omega)$ of the residual phase error $\varepsilon(k)$ obtained in the closed-loop simulations. The power spectrum obtained with the optimal control approach and the ideal mirror is approximately white.

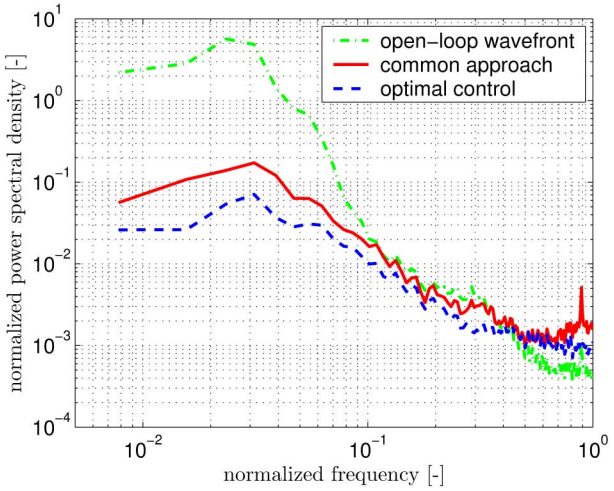

Fig. 7. Normalized averaged power spectrum $P(\omega)$ residual wavefront for closed-loop simulations with realistic DM model.

This means that, at least on average, there is no temporal correlation in the residue that can be used to further improve the performance of the controller. The residue obtained with the common AO control law on the other hand has a strong coloring and shows that there is still plenty of room for improvement. From the power spectra, it is already clear that the residual phase error obtained with the optimal control approach is much smaller than with the common AO control approach. This is confirmed by the performance index J_1. The value of J_1 obtained in the simulations with the ideal DM are $J_1 = 3.27 \times 10^{-3}$ for the common control approach and $J_1 = 1.52 \times 10^{-3}$ for the optimal control approach. This is a reduction of 53.5%. The corresponding values for the simulations with estimated influence matrix of the AO test bench mirror are $J_1 = 3.13 \times 10^{-2}$ and $J_1 = 1.92 \times 10^{-2}$, which corresponds to a reduction of 38.6%. The simulations show that the performance improvement for the simulation with the estimated DM influence matrix is much smaller. Since both simulations differ only in the DM influence matrix, it is clear that in the second scenario the DM fitting error is the limiting factor. As the DM fitting error is not influenced by the controller, it is to be expected that an AO system can only benefit from an advanced control strategy if the DM fitting error is small compared to other error sources. The simulations with the ideal DM show that the proposed control strategy is able to significantly reduce the contribution due to the temporal error. By predicting the future wavefront distortions as $\hat{\varphi}(k+1|k)$, the temporal error caused by the finite time delay between measurement and corrections is reduced. In the AO test bench, the ratio between the fitting and temporal error is very unfavorable because of the relatively small number of DM actuators compared to the number of WFS channels. It is therefore to be expected that the performance gain is larger in AO systems with a smaller fitting error and in situations where the controller related error is more dominant for instance due to an increased turbulence wind speed or higher levels of measurement noise.

VI. Conclusions and Discussion

In this paper, we have presented a data-driven approach to design a controller for rejecting the wavefront distortions in an AO system. The proposed control design strategy is able to take full advantage of the spatio-temporal correlation in the wavefront and consists of two major steps. In the first step open-loop wavefront sensor (WFS) measurements are used to identify a multivariable atmospheric disturbance model. In the second step, the identified atmospheric disturbance model is used to compute the optimal controller.

To identify the multivariable atmospheric disturbance model from the open-loop WFS data, a dedicated subspace identification algorithm has been developed. An important advantage of the proposed subspace algorithm is that it avoids the need for spectral factorization by directly estimating the minimum-phase spectral factor. Since AO systems typically have a large number of WFS channels and the atmospheric disturbance model should describe the full spatio-temporal correlation without assuming any form of decoupling, computational efficiency is an important issue. For this reason, special attention has been paid to reduce the computational demands of the algorithm. The different steps of the algorithm are expressed in terms of the R factor of a single RQ factorization of the stacked block Hankel matrices of past and future data, which is used for data compression. This leads to an efficient implementation both in terms of the number of flops and required memory. The resulting algorithm is able to identify an atmospheric disturbance model for an AO system with up to a few hundred degrees of freedom on a 3 GHz Intel Pentium processor, within a matter of minutes.

An important aspect of the AO control problem is that there is a difference between the objective of minimizing the residual WFS signal and the actual cost function. Given the identified atmospheric disturbance model, the $\mathcal{H}_2$-optimal control framework provides an attractive way to deal with this discrepancy. Formulating the AO problem as a $\mathcal{H}_2$-optimal control problem provides a general strategy for computing the optimal controller. Computing the $\mathcal{H}_2$-optimal controller typically involves the solution to two Riccati equations. By using the Youla parametrization to render the AO control problem into an equivalent feedforward problem, it has been shown that due to the minimum-phase property of the atmospheric disturbance model one of the Riccati equations can be avoided. Furthermore, it has been shown that in the special case that the DM settling time can be neglected with respect to the WFS exposure time an analytical expression for the optimal controller can be derived. The analytical expressions show that optimal controller decomposes wavefront prediction problem followed by a static projection on the actuator space.

The closed-loop controller design procedure obtained by combining the proposed subspace identification algorithm and the analytical solutions to the $\mathcal{H}_2$-optimal control problem, is entirely based on standard matrix operations and provides a noniterative way to go from open-loop measurement data to closed-loop controller design. The proposed control strategy has been demonstrated by means of numerical validation experiments on open-loop WFS data obtained from an experimental setup. The validation experiments show a performance improvement with respect to the common AO control approach.

Under the assumption that the DM is able to take the shape of the estimated wavefront, the use of the proposed control strategy leads to a reduction of the mean-square residual phase error by more than 70%. Using a realistic DM model, the gain in performance for the considered experimental setup reduces to about 14%. The rather drastic reduction in performance can be explained by the relatively large fitting error. In situations where the DM fitting error is not limiting, a large gain in performance is to be expected.

One of the basic assumptions in the data-driven $\mathcal{H}_2$-optimal control approach is that atmospheric wavefront distortions can be modeled as a regular process. Even though this may be a realistic assumption on time-scales in the order of a few minutes, it will fail for longer periods because of gradual changes in the turbulence statistics. This implies that the proposed control strategy has to be extended to guarantee a close to optimal performance over longer time-scales. One way to proceed would be to update the atmospheric disturbance model on a regular basis (see Fig. 2). Ideally, the model updating should be performed in closed-loop to enable continuous operation. This remains a topic for further research. Closely related to this is the issue of robustness with respect to changes in the turbulence statistics. This includes the possible loss in performance due to unmodeled changes like wind gust. Even though a complete robustness analysis is beyond the scope of this paper two observations can be readily made.

First, since the wavefront distortions act as a disturbance input, inaccuracies in the atmospheric disturbance model will never able to destabilize the loop. This implies that stability robustness with respect to turbulence changes will never be an issue. Furthermore, we have seen that the optimal controller can be interpreted as predicting the future distortions followed by a projection on the actuator space. For a single layer of frozen turbulence, it is clear that predicting the future in equivalent to estimating the wavefront at a position in the windward direction. A mismatch between the actual wind speed and the wind speed used to identify the disturbance model can hence be seen as estimating the wavefront at the "wrong" position. Since the common AO control approach entirely neglects the time delay, optimal control is expected to achieve a performance improvement when the velocity mismatch is small compared to the wind speed itself. Even though this is not a proof, it is a clear indicator for a good performance robustness. First simulations on real WFS data seem to confirm this, however, further research is still required.

REFERENCES

[1] M. Brown, M. v. Dam, A. Bouchez, D. L. Migant, R. Cambell, J. Chin, A. Conrad, S. Hartman, E. Johansson, R. Lapon, D. Rabinowitz, P. Stomski, D. Summers, C. Trujillo, and P. Winowich, "Satallites of the largest kuiper belt objects," *Astrophysical J.*, vol. 639, pp. L43–L46, Mar. 2006.

[2] J. Hardy, *Adaptive Optics for Astronomical Telescopes*, ser. Oxford Series in Optical and Imaging Sciences. New York: Oxford Univ. Press, 1998.

[3] R. Tyson, *Principles of Adaptive Optics*, 2nd ed. New York: Academic, 1998.

[4] F. Roddier, *Adaptive Optics in Astronomy*. Cambridge, U.K.: Cambridge Univ. Press, 1999.

[5] M. Born and E. Wolf, *Principles of Optics: Electromagnetic Theory of Propagation*, 7th ed. Cambridge, U.K.: Cambridge Univ. Press, 1999.

[6] M. v. Dam, D. L. Mignant, and B. Macintosh, "Performance of keck observatory adaptive optics system," *Appl. Opt.*, vol. 43, no. 29, pp. 5458–5467, Oct. 2004.

[7] N. Law and R. Lane, "Wavefront estimation at low light levels," *Opt. Commun.*, vol. 126, pp. 19–24, May 1996.

[8] B. Ellerbroek, "Optimizing closed-loop adaptive-optics performance with use of multiple control bandwidths," *J. Opt. Soc. Amer. A*, vol. 11, no. 11, pp. 2871–2886, Nov. 1994.

[9] E. Gendron and P. Léna, "Astronomical adaptive optics," *Astronomy Astrophys.*, vol. 291, pp. 337–347, 1994.

[10] F. Roddier, "Maximum gain and efficiency of adaptive optics systems," *Publications Astronomical Soc. Pacific*, vol. 110, pp. 837–840, Jul. 1998.

[11] C. Dessenne, R.-Y. Madec, and G. Rousset, "Model prediction for closed-loop adaptive optics," *Opt. Lett.*, vol. 22, no. 20, pp. 1535–1537, Oct. 1997.

[12] R. Paschall and D. Anderson, "Linear quadratic gaussian control of a deformable mirror adaptive optics system with time-delayed measurements," *Appl. Opt.*, vol. 32, no. 31, pp. 6347–6358, Nov. 1993.

[13] D. Looze, M. Kasper, S. Hippler, O. B. Ans, and R. Weiss, "Optimal compensation and implementation for adaptive optics systems," *Experimental Astronomy*, vol. 15, no. 2, pp. 67–88, 2003.

[14] B. L. Roux, J.-M. Conan, C. Kulcsár, H.-F. Raynaud, L. Mugnier, and T. Fusco, "Optimal control law for classical and multiconjugate adaptive optics," *J. Opt. Soc. Amer. A*, vol. 21, no. 7, pp. 1261–1276, Jul. 2004.

[15] D. Gavel and D. Wiberg, "Towards strehl-optimizing adaptive optics controllers," in *Adaptive Optical System Technologies II*, ser. Proceedings of SPIE, P. Wizinowich and D. Bonaccini, Eds. : , 2003, vol. 4839, pp. 890–901.

[16] J. Gibson, C. Chang, and B. Ellerbroek, "Adaptive optics: Wave-front correction by use of adaptive filtering and control," *Appl. Opt.*, vol. 39, no. 16, pp. 2525–2537, Jun. 2000.

[17] B. D. O. Anderson and J. B. Moore, *Optimal Filtering*. Englewood Cliffs, NJ: Prentice-Hall, 1979.

[18] L. Ljung and T. Glad, *Modeling of Dynamic Systems*. Englewood Cliffs, NJ, USA: Prentice-Hall, 1994.

[19] M. Jansson, "Subspace identification and arx modeling," in *Proc. 13th IFAC Symp. Syst. Identification*, 2003, pp. 1625–1630.

[20] P. Van Overschee and B. De Moor, "Subspace algorithms for the stochastic identification problem," *Automatica*, vol. 29, no. 3, pp. 648–660, May 1993.

[21] A. Lindquist and G. Picci, "Canonical correction analysis, approximate covariance extension and identification of stationary time series," *Automatica*, vol. 32, no. 5, pp. 709–733, May 1996.

[22] J. Mari, P. Stoica, and T. McKelvey, "Vector arma estimation: A reliable subspace approach," *IEEE Trans. Signal Process.*, vol. 48, no. 7, pp. 2092–2104, Jul. 2000.

[23] K. Peternell, W. Scherrer, and M. Deistler, "Statistical analysis of novel subspace identification methods," *Signal Process.*, vol. 52, pp. 161–177, 1996.

[24] M. Verhaegen, "Identification of the deterministic part of mimo state space models given in innovations from input-output data," *Automatica*, vol. 30, no. 1, pp. 61–74, Jan. 1994.

[25] N. Mastronardi, D. Kressner, V. Sima, P. Van Dooren, and S. Van Huffel, "A fast algorithm for subspace state-space system identification via exploitation of the displacement structure," *J. Computational Appl. Math.*, vol. 132, no. 1, pp. 71–81, Jul. 2001.

[26] D. Bauer, "Choosing integer parameters in subspace methods: A survey on asymptotic results," in *Proc. IFAC Symp. Syst. Identification*, 2003, pp. 1778–1783.

[27] W. Arnold and A. Laub, "Generalized eigenproblem algorithms and software for algebraic Riccati equations," *Proc. IEEE*, vol. 72, no. 12, pp. 1746–1754, Dec. 1984.

[28] T. Chen and B. Francis, *Optimal Sampled-Data Control Systems*. Berlin, Germany: Springer-Verslag, 1995.

[29] K. Zhou, J. Doyle, and K. Glover, *Robust and Optimal Control*. Englewood Cliffs, NJ, USA: Prentice-Hall, 1996.

[30] M. Morari and Zafiriou, *Robust Process Control*. Englewood Cliffs, NJ: Prentice-Hall, 1989.

[31] D. Youla, J. Bongiorno, and H. Jabr, "Modern Wiener-Hopf design of optimal controllers-part II: The multivariable case," *IEEE Trans. Autom. Control*, vol. 21, no. 6, pp. 319–338, Jun. 1976.

[32] M. Vidyasagar, *Control systems synthesis: A factorization approach*. Cambridge, MA: MIT, 1988.

[33] G. Goodwin, S. Graebe, and M. Salgado, *Control System Design*. Englewood Cliffs, NJ: Prentice-Hall, 2001.

Karel Hinnen was born in The Netherlands, on July 23, 1977. He received the M.Sc. degree (*cum laude*) in applied physics from the University of Twente, Enschede, The Netherlands, in 2002, and the Ph.D. degree (*cum laude*) from the Delft University of Technology, Delft, The Netherlands, in 2007.

After working as a Research Assistant, he became involved in a Ph.D. project at what is now known as the Delft Center for Systems of Control. This project was concerned with the development of advanced control strategies for adaptive optics. Currently, he is active as a Research Scientist with Philips Research.

Michel Verhaegen received the Eng. degree in aeronautics from the Delft University of Technology, Delft, The Netherlands, in 1982, and the Ph.D. degree in applied sciences from the Catholic University Leuven, Leuven, Belgium, in 1985.

From 2001 on, he has been appointed a full time Professor with the Delft University of Technology, where he was one of the founders of the new Delft Center for Systems and Control. He is leading long term research projects sponsored by the European Community, the Dutch National Science Foundation (STW) and the Dutch industry. From 1985 on, he held different research positions with NASA, TU Delft, Uppsala, McGill, Lund, and the German Aerospace Laboratory. In 1999, he became Professor with the Department of Systems and Control Engineering, Faculty of Applied Physics, University of Twente, Twente, The Netherlands.

Niek Doelman was born in The Netherlands in 1964. He received the M.Sc. degree (*cum laude*) in applied physics and the Ph.D. degree from the Delft University of Technology, Delft, The Netherlands, in 1987 and 1993, respectively.

Currently, he is a Senior Scientist with the Department of Industrial Modeling and Control, TNO Science and Industry, Delft, the Netherlands. His main research activities include the design and implementation of advanced motion control systems for high precision applications in space, lithography, astronomy, and robotics. His research interests include adaptive filtering and control, active vibration control, adaptive optics, and mechatronics.